Vid22p, a novel plasma membrane protein, is required for the fructose-1,6-bisphosphatase degradation pathway

C. Randell Brown*, Jameson A. McCann*, Graham Guo-Chiuan Hung, Christopher P. Elco and Hui-Ling Chiang‡

Department of Cellular and Molecular Physiology, Pennsylvania State College of Medicine, 500 University Drive, Hershey, PA 17033, USA
*Both authors contributed equally to this work
‡Author for correspondence (e-mail: hlchiang@psu.edu)

Accepted 30 October 2001
Journal of Cell Science 115, 655-666 (2002) © The Company of Biologists Ltd

Summary

Fructose-1,6-bisphosphatase (FBPase), an important enzyme in the gluconeogenic pathway in *Saccharomyces cerevisiae*, is expressed when cells are grown in media containing a poor carbon source. Following glucose replenishment, FBPase is targeted from the cytosol to intermediate Vid (vacuole import and degradation) vesicles and then to the vacuole for degradation. Recently, several *vid* mutants that are unable to degrade FBPase in response to glucose were identified. Here, we present *VID22*, a novel gene involved in FBPase degradation. *VID22* encodes a glycosylated integral membrane protein that localizes to the plasma membrane. Newly synthesized Vid22p was found in the cytoplasm and then targeted to the plasma membrane independent of the classical secretory pathway. A null mutation of *VID22* failed to degrade FBPase following a glucose shift and accumulated FBPase in the cytosol. Furthermore, the majority of FBPase remained in a proteinase K sensitive compartment in the *Δvid22* mutant, implying that *VID22* is involved in FBPase transport from the cytosol to Vid vesicles. By contrast, starvation-induced autophagy and peroxisome degradation were not impaired in the *Δvid22* mutant. This strain also exhibited the proper processing of carboxypeptidase Y and aminopeptidase I in the vacuole. Therefore, Vid22p appears to play a specific role in the FBPase trafficking pathway.

Key words: Vid vesicles, Vacuole, Fructose-1,6-bisphosphatase, *VID* genes

Introduction

The vacuole of *Saccharomyces cerevisiae* is homologous to the mammalian lysosome and is essential for several cellular processes including ph maintenance, osmoregulation, and protein degradation (Klionsky et al., 1990; Jones, 1991; Bryant and Stevens, 1998). The proper function of the vacuole depends upon the targeting of a number of vacuole resident proteins into this organelle. For example, the hydrolase carboxypeptidase Y (CPY) is transported through the secretory pathway to the vacuole by the Vps pathway. This process requires the participation of more than 40 *VPS* genes (Rothman and Stevens, 1986; Johnson et al., 1987; Valls et al., 1987; Robinson et al., 1988; Raymond et al., 1992; Marcusson et al., 1994; Cooper and Stevens, 1996).

Extracellular material and plasma membrane proteins can be internalized and targeted to the vacuole via endocytosis (Hicke, 1997). Proteins can also be delivered from the cytoplasm into the vacuole (Klionsky et al., 1992; Harding et al., 1995; Harding et al., 1996). Two enzymes, aminopeptidase I (API) and α-mannosidase, are synthesized as inactive enzymes within the cytoplasm and are transported from the cytoplasm to the vacuole independent of the secretory pathway (Yoshihisa and Anraku, 1990; Klionsky et al., 1992; Scott et al., 1996). Targeting of API to the vacuole is mediated by the Cvt pathway, a pathway that shares common components with the macroautophagy pathway and the pexophagy pathway (Klionsky and Ohsumi, 1999; Kim and Klionsky, 2000).

A number of circumstances such as changes in nutrient conditions can induce the trafficking of proteins and organelles to the vacuole (Tuttle and Dunn, 1995; Klionsky and Ohsumi, 1999; Kim and Klionsky, 2000). For example, peroxisomes are targeted to the vacuole for degradation when *S. cerevisiae* are shifted from media containing oleic acid to media containing glucose (Chiang et al., 1996), while autophagosomes are formed and targeted to the vacuole when *S. cerevisiae* are starved of nitrogen (Takeshige et al., 1992; Tsukada and Ohsumi, 1993; Klionsky and Ohsumi, 1999; Kim and Klionsky, 2000). Yeast cells deliver the enzyme fructose-1,6-bisphosphatase (FBPase) to the vacuole for degradation following a shift from low to high glucose conditions (Chiang and Schekman, 1991; Chiang et al., 1996; Shieh and Chiang, 1998). Prior to its entry into the vacuole, however, FBPase is targeted to a novel type of Vid vesicle (Huang and Chiang, 1997).

A number of genes are known to play important roles in the FBPase degradation pathway (Hoffman and Chiang, 1996). Previously, we identified *VID24* and determined that this gene is required for the proper targeting of FBPase from Vid vesicles to the vacuole. *VID24* encodes a peripheral membrane protein that associates with the surface of Vid vesicles. In the absence of *VID24*, FBPase remains sequestered within Vid vesicles and

is unable to traffic to the vacuole (Chiang and Chiang, 1998). Here we describe another novel gene, *VID22*, that is essential for FBPase degradation. *VID22* encodes an integral membrane protein that localizes to the plasma membrane. In comparison with wild-type cells, *Δvid22* degraded FBPase at a significantly reduced rate following a glucose shift. The majority of FBPase accumulated in the cytosol in this mutant, suggesting that Vid22p is involved in the targeting of FBPase into Vid vesicles. By contrast, processing of CPY or API to the vacuole was not impaired in the *Δvid22* mutant. Likewise, there was no defect in either starvation-induced autophagy or peroxisome degradation in the *Δvid22* mutant. Therefore, *VID22* appears to play a specific role in the FBPase trafficking pathway.

Materials and Methods

Strains and antibodies

Strains used for this study were: HLY223 (*Matα his3-Δ200 ura3-52 leu2,3-112 trp1-1*), *vid22-1* (*Matα his3-Δ200 ura3-52 leu2,3-112 trp1-1 vid22-1*), Y05282 (*MATa, his3Δ1, leu2Δ0, met15Δ0, ura3Δ0 vid22::kanmx4*) (Euroscarf, Germany), BY4711 (*MATa, his3Δ1, leu2Δ0, met15Δ0, ura3Δ0*) (Euroscarf, Germany), HLY227 (*Matα his3-Δ200 ura3-52 leu2,3-112 vid24::TRP1*), HLY195 (*Matα his3-Δ200 ura3-52 leu2,3-112 pep4::TRP1*), YKK126 (*Matα his3 ura3 leu2 trp1 apg1::LEU2*), HLY810 (*Matα his3-Δ200 ura3-52 leu2,3-112 trp1-1, VID22-V5::URA3*), HLY892 (*Matα his3-Δ200 ura3-52 leu2,3-112 pep4::TRP1 VID22-V5::URA3*) and HLY895 (*Matα ura3-52 leu2,3-112 suc2, sec18-1, VID22-V5::URA3*).

Mouse monoclonal anti-V5 antibodies were purchased from Invitrogen (Invitrogen, Carlsbad CA). Rabbit polyclonal antibodies directed against FBPase, CPY, Pma1p, Vid24p and enolase were produced by Berkeley Antibody Company (Berkeley, CA). HRP-conjugated goat anti-rabbit and HRP conjugated goat anti-mouse antibodies were purchased from Amersham Pharmacia Biotech (Uppsala, Sweden). The enhanced chemiluminescence kit was from NEN (NEN Life Sciences, Boston, MA). Antibodies were used at 1:5000 dilution for V5 and Sec21p and 1:10,000 dilution for FBPase, CPY, Pma1p, dipeptidyl aminopeptidase B (DPAP B), Mnn1p, Pep12p, enolase, HRP-conjugated goat anti-rabbit and HRP conjugated goat anti-mouse.

Isolation of the *vid22-1* mutant

The gene encoding Vid22p was identified using a Tn-lacz/Leu2-mutagenized library provided by Michael Snyder (Yale University, New Haven, CT). This library was amplified in *E. Coli*, purified, and restriction digested with *Not*I. Excised DNA fragments were purified, transformed into HLY223 using a lithium acetate protocol, and plated onto leucine drop-out plates for 5-7 days at 22°C. Mutants were replica plated (colony-blotted) onto nitrocellulose membranes, which were then immersed in SD (with 5% dextrose) for 3 hours at 37°C. Cells were lysed and blotted with affinity purified anti-FBPase antibodies (1:1000 dilution). Membranes were incubated with alkaline phosphatase-conjugated goat anti-rabbit antibodies (1:5000 dilution), and proteins were visualized using color development reagents (Bio-Rad, Richmond, CA). FBPase degradation deficient mutants were identified as dark purple colonies and were selected for further characterization.

Sequencing and cloning of the *VID22* gene

The Tn disrupted genes were identified with a vectorette PCR protocol. A 10 ml culture of the *vid22-1* strain was harvested and chromosomal DNA was isolated, digested with *Dra*I (10 U), and ligated to annealed DNA bubble primer 3′- GAGAGGGAAGAGAG-CAGGCAAGGAATGGAAGCTGTCTGTCGCAGGAGAGGAAG-5′ and 5′-GACTCTCCCTTCTCGAATCGTAACCGTTCGTACGAGA-ATCGC TGTCCTCTCCTTC-3′. The primers (2-4 μM) were annealed by heating at 65°C for 5 minutes followed by the addition of $MgCl_2$ to 1-2 mM at room temperature. The ligation reaction (30 μl) contained digested chromosomal DNA, 1 μl annealed anchor bubble primers, 1 μl (400 U) ligase and 50 μM ATP. This mixture was incubated at 16°C for 9-24 hours.

The mutated gene was amplified via PCR using primers: 5′-CGAATCGTAACCGTTCGTACGAGAATCGCT-3′ and 5′-CGCCA-GGGTTTTCCCAGTCACGAC-3′ and sequenced in the Penn State College of Medicine Core Facility. The flanking sequences of the transposon exhibited exact identity to open reading frame YLR373C using the BLAST search. This gene, *VID22*, was cloned by PCR with primers: 5′-AGCGGCCGCGGGATGGGGAGAGCGATGGACACA-CAG-3′ and 5′-GAGGCGGCCGCCTGGAAGATACTGACTTGC-3′. The PCR product was ligated into pyes2.1/V5 His-TOPO plasmid and transformed into TOP10F′ cells (Invitrogen, Carlsbad, CA). The *VID22* gene was fused in-frame with a sequence encoding a V5 epitope as confirmed via PCR. The fusion gene was excised from the plasmid with *Pvu*II and *Xba*I and ligated into the *Sma*I/*Xba*I site of a digested YIP352 plasmid. The construct was cloned, linearized with *sa*li and integrated into HLY223 using the lithium acetate protocol. This integration resulted in the expression of the Vid22p-V5 fusion protein under the control of the endogenous *VID22* promoter. The second unfused gene has no promoter and should not be expressed. The integration was confirmed by PCR reactions and the expression of Vid22p-V5 was examined by western blotting of total lysates with anti-V5 antibodies.

Characterization of Vid22p

Vid22p-V5 wild-type cells were grown for 2 days in media containing low glucose and then shifted to media containing 2% glucose for the indicated times. Cells were homogenized as described (Chiang and Chiang, 1998). Total extracts were centrifuged at 1000 ***g*** and resuspended in either 50 μl TE buffer (10 mM Tris, 1 mM EDTA, pH 8.0), 50 μl TE with 0.1M Na_2CO_3 (pH 11.5) or 2% Triton X-100. Suspensions were incubated at 4°C for 30 minutes and centrifuged at 13,000 ***g*** for 10 minutes. The distribution of Vid22p and Pma1p was examined by western blotting of fractions with antibodies directed against these proteins. For endo H treatments, the 1000 ***g*** cell pellet was resuspended in endo H buffer (50 mM sodium citrate, pH 5.5, 10 mM NaN_3) and incubated at 75°C for 30 minutes. Samples were treated with 5 mU of endo H enzyme and incubated for 16 hours at 37°C. All samples were boiled, resolved by SDS-PAGE, and Vid22p-V5 was detected using western blots with antibodies directed against the V5 epitope. For CON A binding experiments, cells were lysed in CON A buffer (100 mM KPO_4, pH 6.8, 200 mM NaCl, 1 mM $MnCl_2$, 1 mM $CaCl_2$) containing 1% Triton X-100. The lysates were centrifuged at 13,000 ***g*** for 10 minutes and Con A beads were added to the resultant supernatants. Following a 60 minute incubation, the beads were pelleted and the unbound material (supernatant) was subjected to TCA precipitation. The CON A beads were washed with CON A buffer and the bound material was eluted using SDS sample buffer.

Pulse-chase analysis of Vid22p

To investigate the processing of Vid22p, a temperature sensitive *sec18-1* strain was transformed with a plasmid containing the *VID22-V5* fusion gene. Cells were grown at 22°C to an OD of 2-3, diluted to OD=0.4 and then re-grown to an OD of 0.8. Cells were spheroplasted and resuspended to 5 OD/ml in media containing yeast nitrogen base (YNB) without ammonium sulfate, without amino acids, with 2% glucose, with 1.2 M sorbitol and supplements. Cells were labeled by the addition of 200 μCi/ml ^{35}S-methionine and

cysteine (Specific activity=10 mCi/ml) for 20 minutes at 37°C. The labeling media were removed and cells were washed and resuspended in the chase media containing excess unlabeled L-methionine and L-cysteine (20 μg/ml). Cells were incubated for 0, 30 and 60 minutes at either 22°C or 37°C. Cells were harvested at each time point and solubilized in 200 μl of IP buffer (50 mM Tris, pH 7.4, 1% SDS, 5 mM EDTA). Samples were diluted to 1 ml with IP dilution buffer (50 mM Tris, pH 7.4, 1% Triton X-100 and 200 mM NaCl) and then centrifuged at 13,000 ***g*** for 20 minutes. Supernatants were immunoprecipitated with 10 μl of anti-V5 antibodies or 5 μl of anti-CPY antibodies, followed by the addition of 50 μl of 50% protein G beads or 50 μl of protein A beads (Pharmacia). Precipitated proteins were separated by SDS-PAGE using 7.5% polyacrylamide gels. These radiolabeled proteins were visualized and quantitated with a phosphorimager (Molecular Dynamics).

To study the effect of glucose on the half-life of Vid22p, we used a wild-type strain expressing the Vid22p-V5 protein. Cells were incubated in labeling media containing 2% ethanol plus 200 μCi/ml ^{35}S-methionine and cysteine for 5 hours (glucose starvation conditions). Cells were washed and then incubated in chase media containing either 2% ethanol or 2% glucose. Cells were harvested at 0, 1 and 2 hours and total lysates were immunoprecipitated with anti-V5 antibodies. Immunoprecipitated material was solubilized in SDS sample buffer, boiled and separated by SDS-PAGE. Radiolabeled proteins were visualized with a phosphorimager.

Differential centrifugation

A 10 ml culture of the Vid22p-V5 strain was grown for 2 days in YPKG. Cells were shifted to YPD for *t*=30 minutes, after which, samples were pelleted at 1000 ***g***. The pellets were resuspended in 200 μl of FBPase lysis buffer (50 mM Hepes-NaOH, 5 mM $MgSO_4$, 40 mM $(NH_4)_2SO_4$, 0.1 mM EDTA, 200 μg/ml phenylmethylsufonyl fluoride) and homogenized as described (Chiang and Chiang, 1998). The yeast lysate was centrifuged at 1000 ***g*** (P1) for 15 minutes at 4°C. Both the low-speed pellet and supernatant were collected. The supernatant was sequentially centrifuged; first at 13,000 ***g*** (P13) for 20 minutes in a desktop centrifuge (American Scientific Products), and then at 100,000 ***g*** (P100) and 200,000 ***g*** (P200) for 2 hours using a Beckman ultracentrifuge and a Beckman TLA 100.2 rotor. Supernatant fractions were TCA precipitated and the resultant pellets were resuspended in 100 μl SDS sample buffer. All samples were boiled, resolved by SDS-PAGE, and examined via western blotting using ECL reactions.

Subcellular distribution of newly synthesized Vid22p

Wild-type cells expressing Vid22p-V5 were labeled for 20 minutes and chased for 0, 30 and 60 minutes at 30°C. Cells were harvested and total lysates were subjected to differential centrifugation as described above. Each fraction was collected, solubilized in 2% Triton X-100 and immunoprecipitated with anti-V5 antibodies. The immunoprecipitated materials were resolved by SDS-PAGE and radiolabeled proteins were visualized using a phosphorimager.

Sucrose density gradients

Sucrose density gradients were constructed by sequential addition of 3 ml 50% sucrose, 2 ml 40% sucrose, 2 ml 35% sucrose, 2 ml 30% sucrose, and 2 ml 20% sucrose in FBPase lysis buffer. A 10 ml culture was grown for 2 days in YPKG and then shifted to YPD for 30 minutes. Cell pellets were resuspended in 200 μl FBPase lysis buffer and broken as described above. The lysates were loaded onto the sucrose gradient and centrifuged at 100,000 ***g*** for 20 hours at 4°C. Following centrifugation, samples were aliquoted from the top in 1 ml fractions and precipitated with 10% TCA. The precipitants were resuspended in 50 μl of SDS sample buffer, resolved using SDS-PAGE, and detected with western blotting and ECL reactions.

Immunofluorescence studies

For immunofluorescence studies, cells were grown to saturation in YPKG and then shifted to YPD. One ml samples were collected at *t*=0, 30, and 60 minutes. Samples were fixed with 200 μl of a 37% formaldehyde solution for 30 minutes at 30°C with moderate shaking. Following fixation, cells were washed with KP (0.1 M potassium phosphate, ph 6.5) and KPS buffer (0.1 M potassium phosphate, pH 6.5, 1.2 M sorbitol). Cells were spheroplasted by resuspension in 1 ml of KPS buffer containing 10 μl of β-mercaptoethanol and lyticase (20 U/OD). Following a 60 minute incubation at 30°C, cells were washed, resuspended in KPS buffer and adsorbed to multiwell slides pre-coated with 1% poly-lysine. Samples were blocked with PBST (0.04 M potassium phosphate monobasic, 0.01 M potassium phosphate dibasic, 0.15 M NaCl, 0.1% Tween-20, 10 mg/ml BSA and 0.1% sodium azide) for 15 minutes at 25°C, and incubated with anti-V5 or anti-Pma1p antibodies overnight at 4°C. The primary antibodies were removed and cells were washed four times with PBST. They were then incubated with FITC-conjugated goat anti-mouse or anti-rabbit antibodies for 1 hour at 25°C. The cells were washed four times with PBST and the slides were sealed with mounting media. Cells were examined using a Zeiss Axiovert s100 (Carl Zeiss Inc., Thornwood, NY) fluorescence microscope equipped with a digital camera (Hamamatsu Inc., Japan).

Miscellaneous assays

Degradation of FBPase was performed as described (Hoffman and Chiang, 1996). Briefly, wild-type cells, *vid22-1* mutants, *Δvid22* mutants or mutant strains transformed with the *VID22* gene were grown in media containing low glucose to induce FBPase and then shifted to media containing glucose for the indicated times. The degradation of peroxisomes was examined using 3-oxoacyl Co A thiolase as a marker (Chiang et al., 1996). For proteinase K experiments, total lysates from the *Δvid22* strain were digested with proteinase K (1 mg/ml) in the absence or presence of 2% Triton X-100 for 20 minutes. The reactions were terminated by TCA precipitation and samples were boiled, resolved by SDS-PAGE and analyzed via western blotting. Vid24p induction and distribution were examined as described (Shieh et al., 2001). Cells were shifted to glucose for the indicated time and total lysates were immunoblotted with anti-Vid24p antibodies. For Vid24p distribution experiments, cells were shifted to glucose for 60 minutes and lysed. Samples were first centrifuged at 13,000 ***g*** for 20 minutes and the 13,000 ***g*** supernatants (total) were centrifuged at 200,000 ***g*** for 2 hours. The 200,000 ***g*** supernatant (high-speed supernatant) and 200,000 ***g*** pellet (high-speed pellet) were immunoblotted with anti-Vid24p antibodies as described (Shieh et al., 2001). Processing of CPY and API was performed as described previously (Rothman and Stevens, 1986; George et al., 2000). Starvation-induced autophagy studies were conducted as described previously (Shintani et al., 2001).

Results

FBPase degradation requires the *VID22* gene

The gluconeogenic enzyme FBPase is induced when *S. cerevisiae* cells are starved of glucose. Following glucose replenishment, however, FBPase is targeted to Vid vesicles and then to the vacuole for degradation (Chiang and Schekman, 1991; Huang and Chiang, 1997). A number of FBPase degradation deficient mutants were identified from cells transformed with a Tn-lacz/LEU2 mutagenized library. The cells were colony blotted using anti-FBPase antibodies and alkaline phosphatase-conjugated secondary antibodies. Following color development, mutants were selected as dark

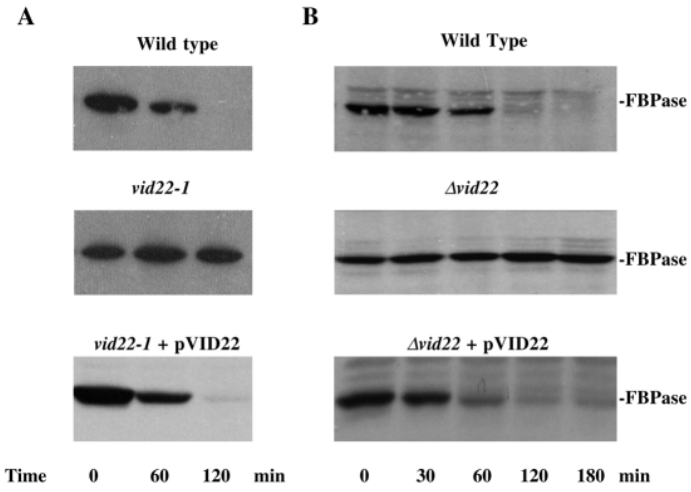

Fig. 1. The *VID22* gene is necessary for FBPase degradation. (A) Wild-type cells, the *vid22-1* transposon mutants and *vid22-1* mutants transformed with the *VID22* gene were grown in synthetic medium containing low glucose for 2 days to induce FBPase. FBPase degradation was examined after cells were shifted to medium containing 2% glucose for 0, 60 and 120 minutes. (B) FBPase production was induced in wild-type cells, *Δvid22* mutants and *Δvid22* mutants transformed with the *VID22* gene. These cells were shifted to glucose for *t*=0, 30, 60, 120 and 180 minutes and the degradation of FBPase was examined.

purple colonies, caused by high immunoreactivity to anti-FBPase antibodies. Using this colony blotting method, we isolated *vid22-1*, a mutant defective in FBPase degradation. The *vid22-1* strain accumulated FBPase when grown in media containing low glucose. However, this strain failed to degrade FBPase following a glucose shift. FBPase remained at 90% of its original level after a glucose shift for 120 minutes (Fig. 1A). By contrast, the wild-type strain completely degraded FBPase during the same time period (Fig. 1A).

Partial sequences of the Tn disrupted *vid22-1* gene were obtained using a vectorette PCR protocol described in Materials and Methods. Sequence analysis indicated that the transposon was inserted at nucleotide residue 224 in the open reading frame of YLR373C as determined by a BLAST search of the *Saccharomyces* Genome Database. A role for *VID22* in FBPase degradation was confirmed via complementation experiments. When the *VID22* gene was cloned and transformed into the *vid22-1* mutant, the FBPase degradation rate was restored to that seen in wild-type cells (Fig. 1A).

To further verify that *VID22* participates in the FBPase degradation process, we used a yeast strain in which open reading frame YLR373C was completely deleted (*Δvid22*). Wild-type cells rapidly degrade FBPase when they are shifted from low glucose to high glucose-containing media. Accordingly, there was a significant decrease in FBPase levels in the wild-type strain at *t*=60 minutes and little if any detectable levels of FBPase at *t*=120 minutes (Fig. 1B). Conversely, the *Δvid22* cells exhibited relatively little change in the level of FBPase over the entire time period when shifted to glucose rich media. When *Δvid22* cells were transformed with the *VID22* gene, their ability to degrade FBPase was restored (Fig. 1B). Thus, *VID22* must play some important role in the FBPase degradation process.

Cells lacking *VID22* accumulate FBPase in the cytosol

Various FBPase degradation deficient mutants accumulate FBPase either within the cytosol or within Vid vesicles (Hoffman and Chiang, 1996; Chiang and Chiang, 1998). This suggests that mutants can be defective either in the import of FBPase into Vid vesicles or in the trafficking of Vid vesicles to the vacuole. To determine the point at which the FBPase

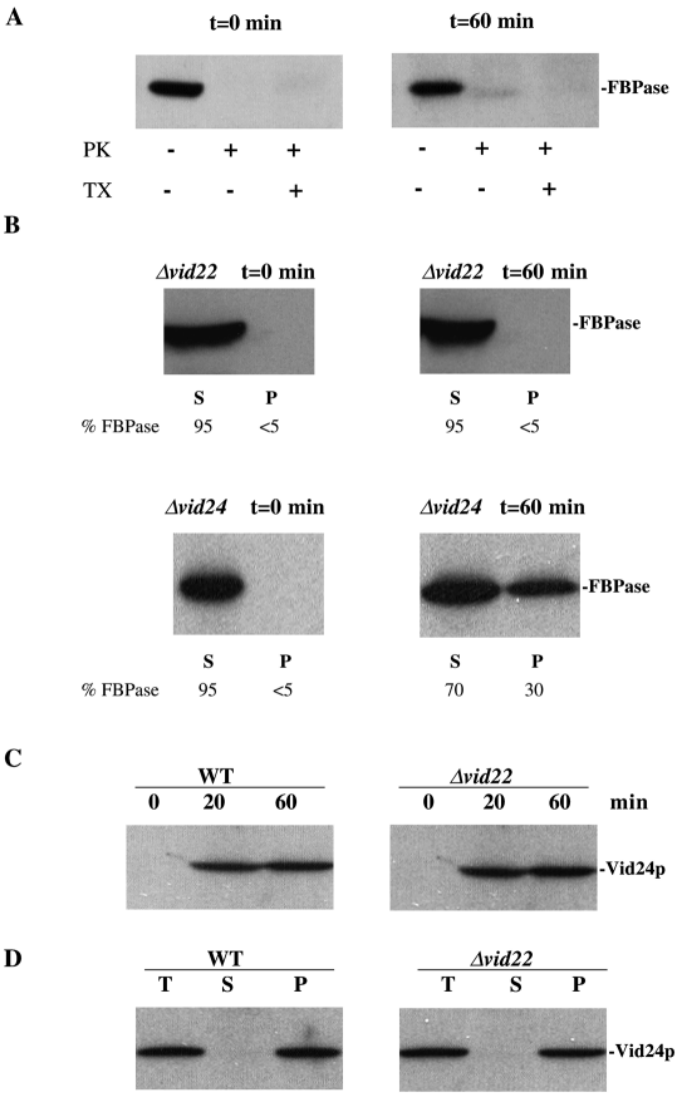

Fig. 2. FBPase accumulates in the cytosol in the *Δvid22* mutant. (A) The *Δvid22* mutant was glucose starved and then shifted to glucose for *t*=0 or *t*=60 minutes prior to harvest. Total lysates were subjected to proteinase K (PK) digestion in the absence or presence of 2% Triton X-100 (TX). (B) Both *Δvid22* and *Δvid24* strains were glucose starved and then shifted to glucose-rich media for 60 minutes. Cells were homogenized and subjected to differential centrifugation. The percentage of FBPase found in each fraction is indicated. (C) Wild-type cells and the *Δvid22* mutant strains were shifted to glucose for 0, 20 and 60 minutes and harvested. Total lysates were immunoblotted with anti-Vid24p antibodies. (D) Wild-type and *Δvid22* mutant strains were shifted to glucose for 30 minutes and harvested. Differential centrifugation was performed. Proteins from the total (T), high-speed supernatant (S) and high-speed pellet (P) fractions were immunoblotted with anti-Vid24p antibodies.

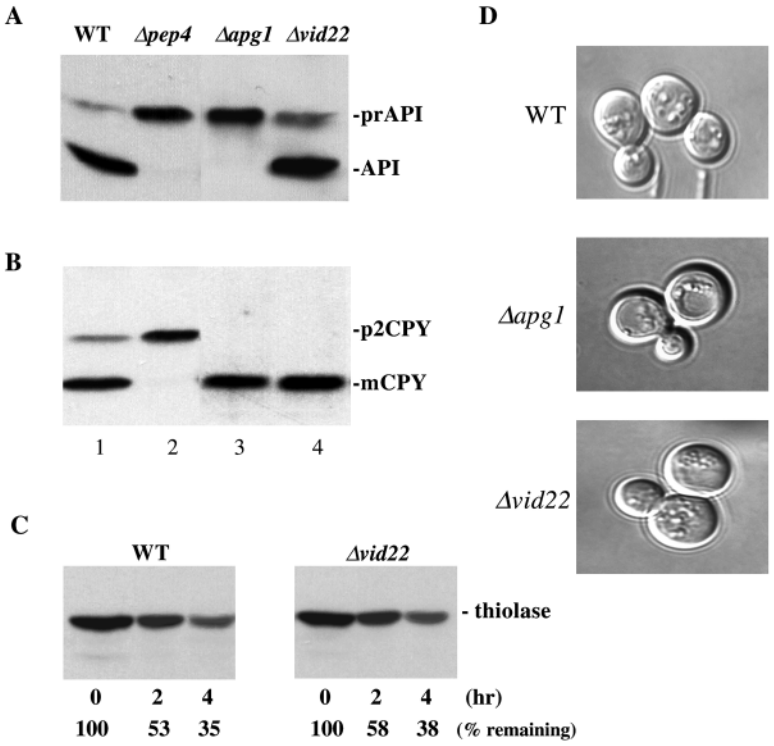

Fig. 3. *VID22* is not required for other vacuolar trafficking pathways. Wild-type, *Δpep4*, *Δagp1* and *Δvid22* strains were grown to log phase and examined for the processing of API and CPY. (A) Processing of API in wild-type (lane 1), *Δpep4* (lane 2), *Δagp1* (lane 3) and *Δvid22* (lane 4) strains. (B) Processing of CPY in wild-type (lane 1), *Δpep4* (lane 2), *Δagp1* (lane 3) and *Δvid22* (lane 4) strains. (C) The degradation of peroxisomes in response to glucose was examined using thiolase as a marker protein. Peroxisomes were degraded with similar kinetics in both the wild-type and *Δvid22* strains. (D) Wild-type, *Δagp1* and *Δvid22* strains were incubated for 6 hours in SD(–N) containing 1 mm PMSF to induce the autophagy pathway. The accumulation of autophagic bodies was observed by light microscopy.

degradation pathway is blocked in the *Δvid22* mutant, we examined FBPase distribution following differential centrifugation and proteinase K treatment assays. The *Δvid22* mutant cells were glucose starved and then shifted to glucose for *t*=0 or *t*=60 minutes. Cells were homogenized and total lysates were subjected to proteinase K digestion in the absence or presence of Triton X-100 (Fig. 2A). At *t*=0 minutes, FBPase was degraded by proteinase K whether Triton X-100 was present or not, suggesting that FBPase was in a proteinase K sensitive compartment, most likely the cytosol. At *t*=60 minutes, FBPase was also sensitive to proteinase K in the presence or absence of Triton X-100 (Fig. 2A). Since FBPase remained in the proteinase K sensitive cytosolic compartment following a glucose shift in the *Δvid22* mutant, these results suggest that the targeting of FBPase from the cytosol to Vid vesicles is blocked in this mutant.

The site of blockage in the FBPase degradation pathway in the *Δvid22* mutant was further examined by differential centrifugation experiments. Glucose starved cells were shifted to glucose containing media for *t*=0 or *t*=60 minutes and then harvested. Cell lysates were subjected to differential centrifugation procedures and FBPase distribution in these fractions was examined. In the *Δvid22* mutant, FBPase was detected in the supernatant fractions, while only a minor amount of FBPase was found in the Vid vesicle pellet fraction (Fig. 2B). Note that the distribution of FBPase in the supernatant versus the pellet fractions did not change from *t*=0 to *t*=60 minutes, suggesting that the absence of Vid22p results in a defect of FBPase targeting to Vid vesicles. By contrast, the *Δvid24* mutant strain did exhibit a change in FBPase localization following a glucose shift. FBPase was found primarily in the supernatant fraction at *t*=0 minute in this mutant. However, FBPase accumulated within the Vid vesicle fraction after a shift of this mutant to glucose for 60 minutes (Fig. 2B). This was as expected, since *Δvid24* has previously been shown to be defective in the trafficking of Vid vesicles to the vacuole, an occurrence that results in the accumulation of FBPase within Vid vesicles (Chiang and Chiang, 1998).

A defect in FBPase targeting to the Vid vesicle fraction could result from either an absence or a reduction in the level of Vid vesicles. Therefore, we examined whether Vid vesicle formation was affected in the *Δvid22* mutants using the Vid vesicle-specific marker Vid24p. When glucose starved cells are replenished with fresh glucose, Vid24p is induced and localizes to Vid vesicles (Chiang and Chiang, 1998). As is shown in Fig. 2C, Vid24p was undetectable at *t*=0 minute in wild-type and *Δvid22* total cell lysates. However, this protein was induced to similar levels in both strains following a glucose shift of *t*=20 and *t*=60 minutes. To determine whether Vid24p distribution was altered in the mutant strain, wild-type and *Δvid22* cells were shifted to glucose for 30 minutes. Cells were homogenized and total lysates were subjected to differential centrifugation. Under these conditions, Vid vesicles are enriched in the high-speed pellet fraction, but not in the high-speed supernatant fraction, which is enriched in cytosol (Brown et al., 2000). In wild-type cells, most of the Vid24p was found in the Vid vesicle containing pellet fraction (Fig. 2D). Likewise, in the *Δvid22* mutants, the majority of Vid24p was also found in the Vid vesicle containing fraction (Fig. 2D), suggesting that the formation of Vid vesicles is not impaired in *Δvid22* mutants. Therefore, the *VID22* gene does not appear to play a role in Vid vesicle biogenesis.

VID22 is not required for other vacuolar trafficking pathways

We next examined whether *VID22* is involved in other vacuolar targeting pathways. API is synthesized as a precursor form in the cytoplasm and then targeted to the vacuole by the Cvt pathway. API is then processed to the mature form in the vacuole via a process that is dependent on the *PEP4* gene (Klionsky et al., 1992; Harding et al., 1995; Klionsky and Ohsumi, 1999; Kim and Klionsky, 2000). As is shown in Fig. 3A, the control wild-type cells processed API to the mature form (lane 1). However, a *Δpep4* mutant failed to process API and accumulated the precursor form of API within cells (lane 2). Likewise, the *Δapg1* mutant, which is defective in the Cvt pathway, accumulated the precursor form of API within cells

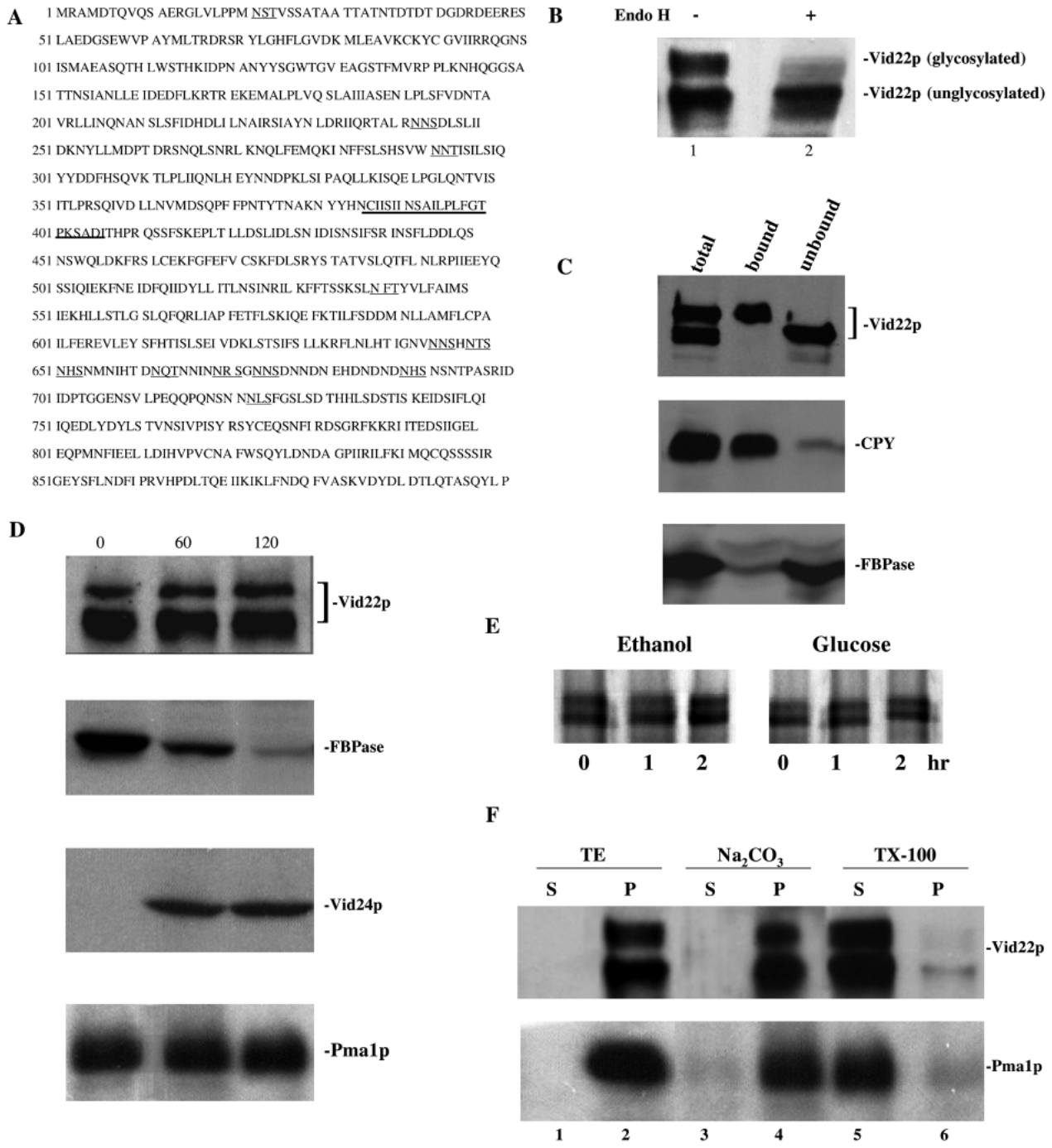

Fig. 4. Vid22p is a glycoslyated integral membrane protein. (A) The predicted amino acid sequence of Vid22p based upon the DNA sequence of YLR373C. Vid22p is a 901 amino acid protein with a predicted molecular weight of 102 kDa and pI of 5.15. Vid22p contains 12 potential N-linked glycosylation sites (underlined regions) and one potential transmembrane domain (bold underlined region). (B) The *VID22* gene was fused with a V5 coding sequence and integrated into a wild-type yeast strain. Vid22p-V5 was detected using SDS-PAGE and western blot analysis with antibodies directed against V5. Vid22p migrated as a doublet representative of glycosylated and unglycosylated forms of Vid22p (lane 1). Lysates were treated with or without endoH to determine whether Vid22p was glycosylated. (C) Cells were lysed in Con A binding buffer and incubated in the presence of Con A beads. The total, bound and unbound materials were examined for the presence of Vid22p, CPY or FBPase via western blot analysis. (D) Cells expressing Vid22p-V5 were grown in low glucose media for 2 days and then shifted to glucose rich media for 0, 60 and 120 minutes. Cells were lysed and examined for the levels of Vid22p, FBPase, Vid24p and Pma1p via western blot analysis. (E) Wild-type cells expressing Vid22p-V5 were labeled in ethanol and chased in the presence of 2% ethanol or 2% glucose. Cells were harvested at 0, 1 and 2 hours and total lysates were immunoprecipitated with anti-V5 antibodies. Radiolabeled Vid22p-V5 was visualized using a phosphorimager. (F) Vid22p-V5 cells were shifted to glucose for 30 minutes. Cells were homogenized and lysates were resuspended in either TE alone, TE containing Na_2CO_3 (ph 11.5) or TE containing 2% TX-100. The distribution of Vid22p and Pma1p in the pellet and the supernatant fractions was examined by western blotting with anti-V5 or anti-Pma1p antibodies.

(lane 3). By contrast, the majority of API was processed to the mature form in the *Δvid22* mutant (lane 4). Therefore, API processing is not impaired in cells lacking the *VID22* gene.

CPY is sorted to the vacuole from the secretory pathway by the Vps targeting pathway (Rothman and Stevens, 1986; Johnson et al., 1987; Valls et al., 1987; Robinson et al., 1988; Raymond et al., 1992; Marcusson et al., 1994; Cooper and Stevens, 1996). In wild-type cells, CPY is synthesized and processed to the p1 form in the ER. CPY is further modified to the p2 form in the Golgi and then processed to the mature form in the vacuole in a process that requires the *PEP4* gene (Klionsky et al., 1990; Jones, 1991; Bryant and Stevens, 1996). As is shown in Fig. 3B, most of the CPY was in the mature form in wild-type cells (lane 1), while the p2 form accumulated in *Δpep4* mutants (lane 2). Note that the *Δapg1* mutant did not affect the maturation of CPY, as indicated by the presence of the mature form of this protein (lane 3). In a similar manner, the *Δvid22* mutant strain processed CPY to the mature form (lane 4). Taken together, these results suggest that the *VID22* gene is not involved in the Vps or Cvt targeting pathways.

Peroxisomes are also targeted to the vacuole for degradation in response to glucose (Chiang et al., 1996). As an indicator of peroxisomal trafficking to the vacuole, we examined the levels of the peroxisomal marker protein 3-oxoacyl Co A thiolase (Fig. 3C). Thiolase expression was induced when wild-type or *Δvid22* cells were grown in media containing oleic acid. However, the levels of thiolase decreased to approximately 35% of the original levels when these same cells were shifted to media containing fresh glucose. This is consistent with our previous results in which a similar percentage of peroxisomes remained after a prolonged shift in glucose (Chiang et al., 1996). Thus, this indicates that *VID22* does not play a role in the trafficking of peroxisomes to the vacuole.

We next examined whether *VID22* might play some essential role in nitrogen starvation induced autophagy. Cells were subjected to nitrogen starvation conditions, in order to induce the formation and trafficking of autophagosomes to the vacuole. To allow for the accumulation of autophagic bodies in the vacuole, cells were treated with PMSF, a compound that inhibits the action of proteinase B. A number of autophagic bodies were observed in the vacuole of wild-type cells following nitrogen starvation (Fig. 3D). The *Δvid22* strain also contained a number of these structures within their vacuoles. By contrast, autophagic bodies were not observed in the vacuole of a strain in which the *APG1* gene was deleted. Therefore, this indicates that *VID22* is not a required component of the autophagy pathway. Taken together, these results suggest that *VID22* plays a specific role in the targeting of FBPase to the vacuole. Accordingly, this gene does not appear to be required for a variety of other vacuolar trafficking processes.

Vid22p is a glycosylated integral membrane protein

VID22 resides on chromosome XII and encodes a protein with the amino acid sequence shown in Fig. 4A. To date, the *VID22* gene product has not been analyzed, although a number of the characteristics of Vid22p can be inferred based upon sequence analysis. Vid22p is a protein of 901 amino acids with a predicted molecular weight of 102 kDa and a pI of 5.15. Based upon Kyle-Doolittle hydropathy and TMpred analysis, Vid22p contains a hydrophobic region that may serve as a transmembrane domain. Furthermore, there are 12 potential N-linked glycosylation sites found in the Vid22p amino acid sequence, suggesting that Vid22p may be a glycoprotein (Fig. 4A). Note that Vid22p does not contain a N-terminal hydrophobic region that might be used as a signal sequence for protein translocation into the ER.

A construct was generated in which a V5 epitope was fused in frame with Vid22p at the C terminus. The *VID22–V5* fusion gene was subcloned into the integration vector YIP352, linearized with *Sal*I, and integrated into the yeast genome. The addition of the V5 tag to Vid22p did not affect the kinetics of FBPase degradation (Fig. 4D). Therefore, this procedure allowed for the detection of Vid22p with antibodies directed against the V5 epitope without compromising the function of this protein. Vid22p was observed as a doublet (Fig. 4B, lane 1). As stated above, Vid22p contains 12 potential glycosylation sites. Therefore, the faster migrating band might represent the unglycosylated form of Vid22p, while the slower migrating band could represent the glycosylated form. To test this, cellular lysates were treated with endo H glycosidase and then examined by western blot. The high molecular weight band appeared to significantly decrease in intensity following endo H glycosidase treatment (Fig. 4B, lane 2). This most likely represents the conversion of glycosylated Vid22p to unglycosylated Vid22p. Similar results were obtained when Vid22p was immunoprecipitated and then treated with endo H (not shown). These results suggest that Vid22p is a glycosylated protein.

To further verify that Vid22p is glycosylated, we tested whether this protein would bind to beads containing covalently crosslinked Con A. Cellular lysates were incubated with Con A beads and the Con A bound and unbound materials were examined via western blot analysis. As controls, we tested for the localization of the glycosylated protein CPY and the unglycosylated protein FBPase. As expected, CPY bound to Con A beads, while FBPase did not. Note that glycosylated Vid22p (the slower migrating band) bound to Con A, while the unglycosylated band (the faster migrating band) did not bind to Con A (Fig. 4C). Therefore, the endo H and Con A binding experiments indicate that the slower migrating band represents the glycoslyated form of Vid22p, while the faster migrating band represents the unglycoslylated form.

We next determined whether Vid22p expression or degradation was affected by the presence of glucose. Wild-type cells expressing Vid22p-V5 were glucose starved and then shifted to glucose-containing media. Cells were harvested and lysates were immunoblotted with anti-V5 antibody to examine the steady state levels of Vid22p. As is shown in Fig. 4D, Vid22p levels did not change in response to glucose, while the levels of FBPase decreased significantly over the same period of time. As an additional control, we examined Pma1p and observed that the levels were not changed. By contrast, Vid24p was induced following a glucose shift, in agreement with previous results (Chiang and Chiang, 1998). To determine whether Vid22p degradation was affected by the presence of glucose, cells expressing Vid22p-V5 were labeled under starvation conditions (ethanol) and then chased for 0, 1 and 2 hours in the presence or absence of glucose. Cells were harvested and Vid22p-V5 was immunoprecipitated using anti-V5 antibodies. There was no significant difference in the levels of radiolabeled Vid22p when cells were chased either in

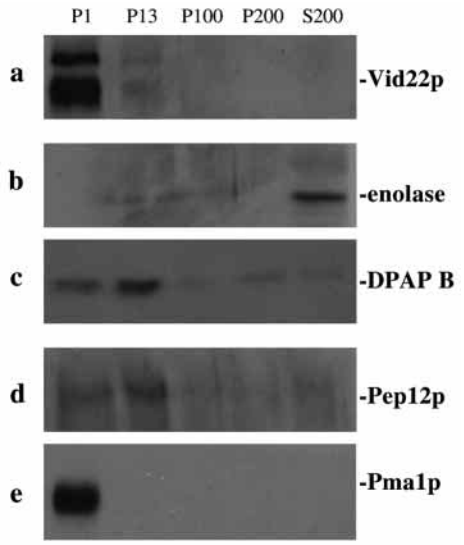

Fig. 5. Vid22p sediments in a low-speed fraction. The Vid22p-V5 strain was glucose starved and then shifted to glucose containing media for 30 minutes. Differential centrifugation of the yeast cellular lysate was used to determine the localization of Vid22p (a). The majority of Vid22p was found to localize within the P1 (low-speed) fraction. A small amount of Vid22p was detected in the P13 fraction. The cytosolic marker enolase was found in the S200 fraction (b). The vacuole marker DPAP B and endosomal marker Pep12p were found primarily in the P13 fraction (c-d). The plasma membrane ATPase Pma1p was localized in the P1 fraction (e).

ethanol or in glucose (Fig. 4E). Thus, Vid22p appears to be a stable protein and its rate of degradation is not accelerated by glucose.

Vid22p contains putative transmembrane domains as determined by Kyte-Doolittle hydropathy plot and TMpred analysis. Therefore, Vid22p may be an integral membrane protein. In order to test this, cells were homogenized and total lysates were subjected to extraction procedures. Samples were resuspended in TE buffer, TE with Na_2CO_3, or TE with 2% Triton X-100. Samples were incubated at 4°C for 30 minutes and then centrifuged. The resultant supernatants and pellets were examined using SDS-PAGE and western blot analysis. As is shown in Fig. 4F, in the presence of TE buffer, Vid22p was associated with the pellet fraction (lane 2) and not the supernatant (lane 1). Likewise, Vid22p remained associated with the pellet fraction (lane 4) when samples were extracted with Na_2CO_3. Following extraction with Triton X-100, however, Vid22p was found in the supernatant fraction (lane 5) but not in the pellet fraction (lane 6). As a control, we examined the effects of these extraction procedures on the distribution of the integral membrane protein Pma1p. Pma1p was extracted into the supernatant fraction by Triton X-100 treatment, but remained in the pellet fraction when samples were treated with TE buffer alone or with Na_2CO_3 (Fig. 4F). Therefore, Vid22p exhibits the same characteristics as an integral membrane protein.

Vid22p is found in plasma membrane-containing fractions

To address whether Vid22p associates with subcellular organelles, we performed a series of differential centrifugation experiments. The majority of Vid22p was found in the P1 low-speed pellet following differential centrifugation (Fig. 5a). Potentially, this fraction could contain cell membranes, nuclei and unbroken cells. To distinguish between these possibilities, we examined the distribution of a number of marker proteins. The cytosolic marker protein enolase was found primarily in the S200 fraction (Fig. 5b), indicating that the majority of cells had been lysed. The vacuolar marker dipeptidyl aminopeptidase B (DPAP B) and the endosomal marker Pep12p (Becherer et al., 1996) were found primarily within the P13 fraction (Fig. 5c,d), while the plasma membrane protein Pma1p was located mainly within the P1 fraction (Fig. 5e). Although a small amount of Vid22p was detected within the P13 fraction, Vid22p was not detected in the P100, P200 and S200 fractions. Taken together, these results indicate that Vid22p is associated with fast sedimenting structures that co-localize with the plasma membrane marker Pma1p.

To further characterize the localization of Vid22p within cells, we subjected the total lysates to centrifugation through a sucrose density gradient. Fractions were collected following centrifugation and the resultant material was examined by western blot analysis using a V5-specific antibody. The majority of Vid22p was found in fractions 7-10 (Fig. 6a). Likewise, most of the Pma1p was localized to these fractions, although a small amount was found in fraction 2 (Fig. 6b). By contrast, the distribution of Vid22p did not overlap with other organelle marker proteins that were examined. For example, the ER-derived COP I vesicle protein Sec21p (Bednarek et al., 1995) was found in fractions 3-4 (Fig. 6c), while the Golgi protein Mnn1p (Graham et al., 1994) and the vacuolar protein CPY were found localized to fractions 1-5 (Fig. 6d,e). There was some overlap between Vid22p and the Vid vesicle marker protein Vid24p (Fig. 6f). However, the Vid22p and Vid24p peaks did not coincide. These results support the contention that Vid22p is a plasma membrane protein, and is not associated with other cellular organelles.

Vid22p is a plasma membrane protein

The localization of Vid22p was further examined via the use of indirect immunofluorescence analysis. Wild-type cells expressing Vid22p-V5 were glucose starved and then incubated in fresh glucose as described above. The cells were fixed and processed for indirect immunofluorescence analysis using the V5-specific antibody. Vid22p appeared to localize to the surface of the cells in a pattern indicative of plasma membrane staining (Fig. 7a-c). This plasma membrane localization was confirmed via staining of cells with an antibody specific for Pma1p. FITC-fluorescence labeling of Pma1p showed similar staining as Vid22p (Fig. 7d-f). Therefore, these immunofluorescence results are consistent with the conclusion that Vid22p is localized within the plasma membrane. Interestingly, the localization of the Vid22p to the plasma membrane remained unchanged following the addition of glucose (Fig. 7a-c).

To test whether Vid22p is endocytosed and delivered to the vacuole in response to glucose, Vid22p distribution was examined in a *Δpep4* mutant strain expressing Vid22p-V5. Cells were shifted to glucose for the indicated times and examined for Vid22p distribution by indirect

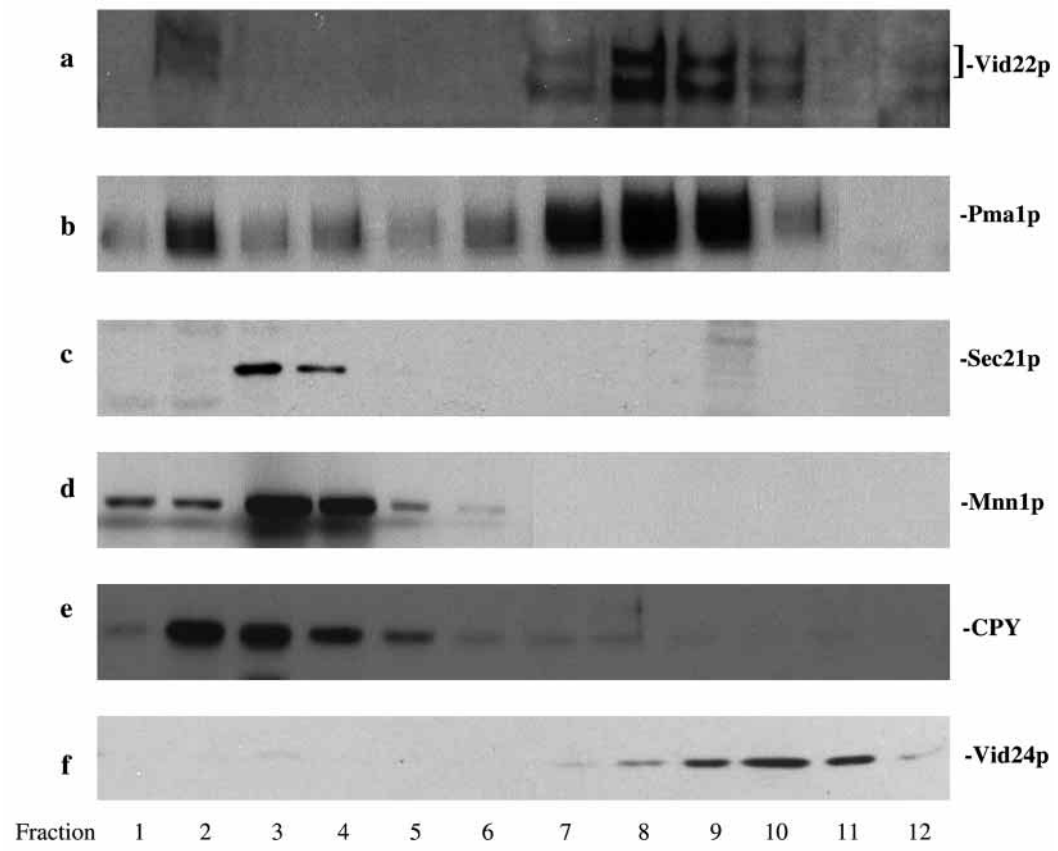

Fig. 6. Vid22p co-localizes with the plasma membrane marker protein, Pma1p. The Vid22p-V5 strain was glucose starved and shifted to fresh glucose media for 30 minutes. Cells were lysed and the total lysate was applied to the top of a 20-50% sucrose gradient. Following a 20 hour spin at 100,000 ***g***, fractions from the sucrose gradient were examined for the distribution of Vid22p (a), the plasma membrane marker Pma1p (b), a COP I vesicle protein Sec21p (c), the Golgi marker Mnn1p (d), the vacuolar protein CPY (e) and the Vid vesicle marker protein Vid24p (f).

immunofluorescence microscopy. Most of the Vid22p staining was found on the plasma membrane, whether *Δpep4* cells were glucose starved or shifted to glucose (Fig. 7g-i). Therefore, the majority of Vid22p appears to remain on the plasma membrane and is not endocytosed in response to glucose.

Vid22p is targeted to the plasma membrane independent of the classical secretory pathway

Most plasma membrane proteins are initially synthesized and translocated into the ER. From there, they then travel through the secretory pathway and to the plasma membrane. If Vid22p is targeted to the plasma membrane via the secretory pathway, then the processing of Vid22p should be inhibited when the secretory pathway is blocked. To test this idea, pulse chase experiments were conducted using a temperature-sensitive *sec18-1* mutant strain that blocks the secretory pathway when incubated at the nonpermissive temperature (Kaiser and Schekman, 1990; Graham and Emr, 1991). A *sec18-1* mutant strain expressing Vid22p-V5 was pulsed at the nonpermissive temperature and chased at either the permissive or nonpermissive temperature for the indicated time points. Cells were harvested and half of the aliquots were immunoprecipitated with anti-V5 antibodies and the other half of the aliquots were immunoprecipitated with anti-CPY antibodies. As expected, CPY was processed to the p1 form, the p2 form and finally the mature form following a chase of the *sec18-1* mutant at the permissive temperature (Fig. 8A). However, CPY remained as the p1 form when the *sec18-1* mutant strains were chased at the nonpermissive temperature. By contrast, Vid22p processing was not inhibited when the *sec18-1* mutant was chased either at the permissive or nonpermissive temperatures (Fig. 8A). Since Vid22p processing was not inhibited when ER-Golgi transport was blocked, Vid22p may not travel through the classical secretory pathway. However, these results do not rule out the possibility that Vid22p glycosylation occurs in the ER.

To determine whether glycosylation of Vid22p occurs in the ER, we examined the distribution of newly synthesized Vid22p using pulse-chase experiments combined with subcellular fractionation (Fig. 8B). Wild-type cells expressing Vid22p-V5 were labeled for 20 minutes and chased at t=0, 30 and 60 minutes. Cells were harvested and total lysates from each time point were subjected to differential centrifugation. To determine the distribution of Vid22p, fractions collected from differential centrifugation were detergent solubilized and immunoprecipitated with an anti-V5 antibody. As is shown in Fig. 8B, newly synthesized Vid22p was in the S200 fraction at t=0 minute. Vid22p appeared as a doublet, but still remained in the S200 fraction following a chase for 30 minutes. However, at t=60 minutes, Vid22p was detected in the plasma membrane fraction (P1). Note that Vid22p was not found in the P13 or P100 fractions that contain vacuole, ER or Golgi at any of the time points. Likewise, Vid22p was detected in the S200 fraction at t=30 minutes and P1 fraction at t=60 minutes, when the *sec18-1* mutant was shifted to the nonpermissive temperature, but not in the ER fraction at any time point in this strain (not shown). This is consistent with the observation that Vid22p does not contain an N-terminal hydrophobic signal sequence for protein translocation into the ER. Therefore, these results suggest that Vid22p is targeted to the plasma membrane independent of the classical secretory pathway.

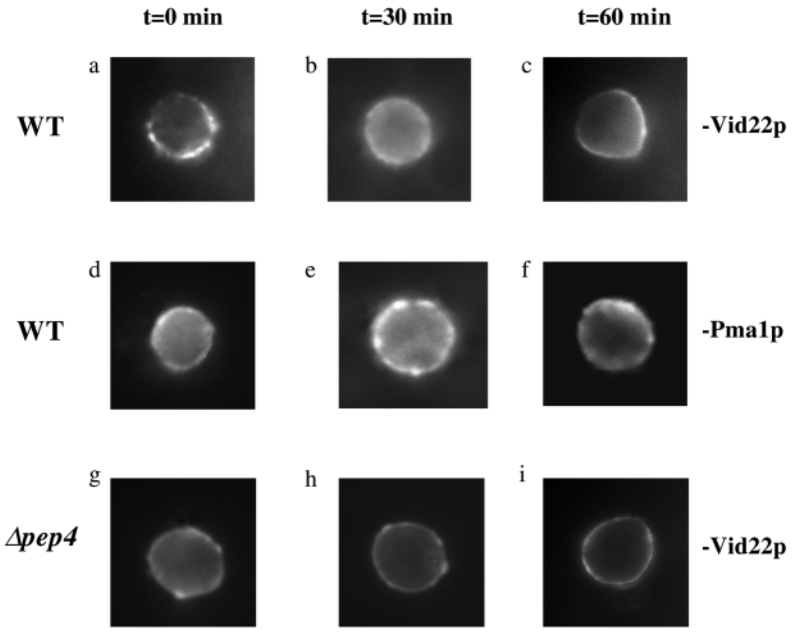

Fig. 7. Vid22p localizes to the plasma membrane. The Vid22p-V5 strain was glucose starved and shifted to fresh glucose media for *t*=0, 30 and 60 minutes. Immunofluorescence microscopy was then used to determine the localization of Vid22p. Staining of Vid22p appeared to be primarily within the plasma membrane in wild-type cells as determined by FITC-fluorescence labeling (a-c). Pma1p, a plasma membrane marker, exhibited FITC-fluorescence staining on the plasma membrane (d-f). In the *Δpep4* strain, the majority of the Vid22p staining was on the plasma membrane either before or after a glucose shift (g-i).

Discussion

FBPase is a key enzyme involved in the gluconeogenic pathway. The synthesis of FBPase is induced when *S. cerevisiae* are grown in media containing a poor carbon source. Following glucose replenishment, however, cells selectively target FBPase from the cytosol into Vid vesicles and then to the vacuole for degradation (Chiang and Schekman, 1991; Huang and Chiang, 1997). During the study of this degradation pathway, we have isolated a number of mutants that fail to degrade FBPase following a glucose shift. Some of these mutants accumulate FBPase within the cytosol, while others accumulate FBPase in Vid vesicles (Hoffman and Chiang, 1996; Chiang and Chiang, 1998). Although a great deal remains to be learned about the biogenesis and function of Vid vesicles, we have performed an initial characterization of these structures. We determined that Vid vesicles are distinct from other known organelles such as vacuoles, ER, Golgi, mitochondria, peroxisomes, endosomes and COP I- and COP II-containing vesicles (Huang and Chiang, 1997).

FBPase degradation-deficient mutants can be defective in one of several steps in the FBPase degradation pathways. Mutations can prevent targeting of FBPase from the cytosol into the Vid vesicle. Additionally, mutations can inhibit trafficking of Vid vesicles to the vacuole. We have shown previously that the *VID24* gene is involved in the second step of the targeting pathway (Chiang and Chiang, 1998). In the present study, we have begun to characterize the *VID22* gene, a gene that encodes a glycosylated integral membrane protein. Subcellular fractionation by differential centrifugation and a sucrose density gradient revealed that Vid22p was distributed in the same fraction as Pma1p, a known plasma membrane marker. Finally, the localization of Vid22p to the plasma membrane was further confirmed via the use of indirect immunofluorescence analysis. Vid22p was localized to

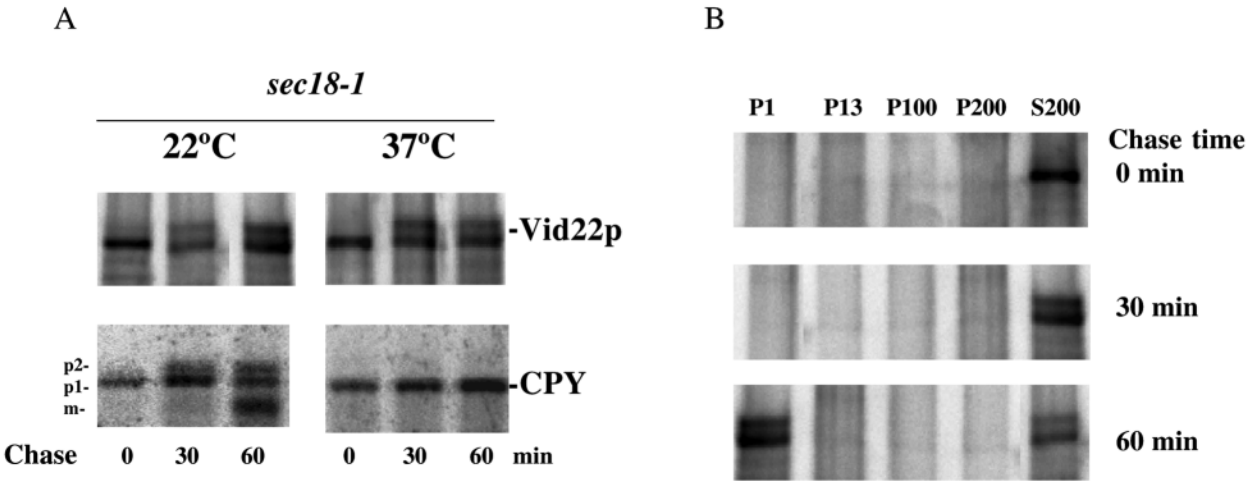

Fig. 8. Vid22p is targeted to the plasma membrane independent of the secretory pathway. (A) The *sec18-1* mutant strain expressing Vid22p-V5 was radiolabeled for 20 minutes at 37°C and chased for 0, 30 and 60 minutes at 22°C or 37°C. Total lysates were immunoprecipitated with anti-V5 antibodies or anti-CPY antibodies. Immunoprecipitated materials were resolved by SDS-PAGE and radiolabeled proteins were visualized using a phosphorimager. (B) Wild-type cells expressing Vid22p-V5 were labeled for 20 minutes and chased for 0, 30 and 60 minutes at 30°C. Cells were lysed and subjected to differential centrifugation as described in the Materials and Methods section. Each fraction was detergent solubilized and immunoprecipitated with an anti-V5 antibody. The precipitated proteins were solubilized in SDS sample buffer and resolved by SDS-PAGE. Radiolabeled Vid22p was visualized by phosphorimager analysis.

the plasma membrane and exhibited a similar staining pattern to cells that were stained with antibodies against Pma1p.

Most plasma membrane proteins and secretory proteins are translocated into the ER and travel through the Golgi prior to their delivery to their final destinations. However, protein export through the non-classical secretory pathway has been demonstrated (Kuchler and Thorner, 1992; Michaelis, 1993; Cleves et al., 1996; Florkiewicz et al., 1998; Boulianne et al, 2000; Dahl et al., 2000). For example, the yeast a-factor is secreted by the non-classical secretory pathway (Michaelis, 1993; Kuchler et al., 1989; Kuchler and Thorner, 1992). Human FGF-2 is also secreted by a mechanism independent of the ER/Golgi pathway (Florkiewicz et al., 1998; Dahl et al., 2000). Mammalian galectins play important roles in diverse biological events and are secreted by the non-classical ER/Golgi pathway (Dodd and Drickamer, 2001). Yeast cells expressing galectin-1 export this protein at a normal rate when the secretory pathway is blocked by the *sec18* mutant at the nonpermissive temperature, suggesting that galectin-1 export uses a new pathway that is distinct from the classical secretory pathway (Cleves et al., 1996). In a similar manner, Vid22p processing was not inhibited by the *sec18-1* mutant, which blocks the secretory pathway at the nonpermissive temperature. Furthermore, Vid22p first appears as a low molecular weight band in the S200 fraction following pulse labeling. The high molecular weight band also appeared in the S200 fraction before Vid22p trafficked to the plasma membrane fraction. Note that Vid22p was not found in the ER or Golgi-containing fractions, suggesting that Vid22p does not travel through the ER/Golgi pathway. Furthermore, there is no hydrophobic N-terminal region that might act as a signal sequence for Vid22p to translocate into the ER. Therefore, these results suggest that Vid22p is delivered to the plasma membrane independent of the ER/Golgi secretory pathway. To the best of our knowledge, Vid22p is the first example of a plasma membrane protein that is targeted from the cytoplasm independent of the classical secretory pathway.

Vid22p was found to play an important role in the degradation of FBPase, since the deletion of *VID22* resulted in a significant decrease in the rate of FBPase degradation. In the *Δvid22* mutant, FBPase accumulated primarily in the cytosolic fraction. This implies that the FBPase degradation defect is at the trafficking step from the cytosol to Vid vesicles. However, the reduced FBPase targeting to Vid vesicles in the *Δvid22* mutants was not due to a decrease in Vid vesicle formation. Instead, the cytosolic component was found to be defective in this strain. We have recently identified cyclophilin A as the cytosolic protein that mediates the function of Vid22p in the FBPase import process (Brown et al., 2001). The levels of Cpr1p were significantly decreased in the *Δvid22* mutant strain compared with wild-type controls. Furthermore, the addition of purified Cpr1p to *Δvid22* in vitro components stimulated the import of FBPase. Therefore, Vid22p regulates the levels of Cpr1p, which in turn stimulates FBPase import into Vid vesicles.

A number of proteins are required to carry out the degradation of FBPase. While we have identified some of these proteins, a clear picture of the individual roles that these proteins play in the process awaits further investigation. The characterization of FBPase degradation mutants will enhance our knowledge of the FBPase degradation pathway. Accordingly, our goals are to identify more genes involved in the FBPase degradation pathway and to determine the mechanisms by which these proteins induce the proper trafficking and degradation of FBPase.

We thank members of the Chiang laboratory for critically reading this manuscript. We thank S. Emr (University of California at San Diego), T. Stevens (University of Oregon), C. Barlowe (Dartmouth Medical School, Hanover, NH), T. Graham (Vanderbilt University), D. Klionsky (U. Michigan) for providing antibodies, Y. Ohsumi (National Institute for Basic Biology, Japan) and R. Schekman (University of California at Berkeley) for yeast strains. We also thank Jill Stahl at the Core Facility, Penn State College of Medicine for sequencing DNA. This work was supported by NIH RO1GM59480 to Hui-Ling Chiang.

References

Becherer, K. A., Reider, S. E., Emr, S. E. and Jones, E. W. (1996). Novel syntaxin homologue, Pep12p, required for the sorting of lumenal hydrolases to the lysosome-like vacuole in yeast. *Mol. Biol. Cell* **7**, 579-594.

Bednarek, S. Y., Ravazzola, M., Hosobuchi, M., Amherdt, A., Schekman, R. and Orci, L. (1995). COPI and COP-II coated vesicles bud directly from the endoplasmic reticulum in yeast. *Cell* **83**, 1183-1196.

Boulianne, R. P., Liu, Y., Aebi, M., Lu, B. C. and Kues, U. (2000). Fruiting body development in Coprinus cinereus: regulated expression of two galectins secreted by a non-classical pathway. *Microbiology* **146**, 1841-1853.

Brown, C. R., McCann, J. A. and Chiang, H.-L. (2000). The Heat Shock Protein Ssa2p is Required for Import of Fructose-1,6-bisphosphatase into Vid Vesicles. *J. Cell Biol.* **150**, 65-76.

Brown, C. R., Cui, D.-Y., Hung, G. G.-C. and Chiang, H.-L. (2001). Cyclophilin A mediates Vid22p function in the import of fructose-1,6-bisphosphatase into Vid vesicles. *J. Biol. Chem.* (in press).

Bryant, N. J. and Stevens, T. H. (1998). Vacuole biogenesis in *Sacharomyces cerevisiae*: Protein transport pathways to the yeast vacuole. *Microbiol. Mol. Biol. Rev.* **62**, 230-247.

Chiang, H.-L. and Schekman, R. (1991). Regulated import and degradation of a cytosolic protein in the yeast vacuole. *Nature* **350**, 313-318.

Chiang, H.-L., Schekman, R. and Hamamoto, S. (1996). Selective uptake of cytosolic, peroxisomal and plasma membrane proteins by the yeast vacuole. *J. Biol. Chem.* **271**, 9934-9941.

Chiang, M.-C. and Chiang, H.-L. (1998). Vid24p, a novel protein localized to the fructose-1,6-bisphosphatase-containing vesicles, regulates targeting of fructose-1,6-bisphosphatase from the vesicles toe the vacuole for degradation. *J. Cell Biol.* **140**, 1347-1356.

Cleves, A. E., Cooper, D. N., Barondes, S. H. and Kelly, R. B. (1996). A new pathway for protein export in Saccharomyces cerevisiae. *J. Cell Biol.* **133**, 1017-1026.

Cooper, A. A. and Stevens, T. H. (1996). Vps10p cycles between the late-Golgi and prevacuolar compartments in its function as the sorting receptor for multiple yeast vacuolar hydrolases. *J. Cell Biol.* **133**, 529-541.

Dahl, J. P., Binda, A., Canfield, V. A. and Levenson, R. (2000). Participation of Na,K-ATPase in FGF-2 secretion: rescue of ouabain-inhibitable FGF-2 secretion by ouabain-resistant Na,K-ATPase alpha subunits. *Biochemistry* **39**, 14877-83.

Dodd, R. B. and Drickamer, K. (2001). Lectin-like proteins in model organisms: implication for evolution of carbohydrate-binding activity. *Glycobiology* **11**, 71R-79R.

Florkiewicz, R. Z., Anchin, J. and Baird, A. (1998). The inhibition of fibroblast growth factor-2 export by cardenolides implies a novel function for the catalytic subunit of Na+, K+-ATPase. *J. Biol. Chem.* **273**, 544-551.

George, M. D., Baba, M., Scott, S. V., Mizushima, N., Garrison, B. S., Ohsumi, Y. and Klionsky, D. (2000). Apg5 functions in the sequestration step in the cytoplasm-to-vacuole targeting and macroautophagy pathways. *Mol. Biol. Cell* **11**, 969-982.

Graham, T. R. and Emr, S. D. (1991). Compartmental organization of Golgi-specific protein modification and vacuolar protein sorting events defined in a yeast sec18 (NSF) mutant. *J. Cell Biol.* **114**, 207-218.

Graham, T. R., Seeger, M., Payne, G., Mackay, V. and Emr, S. (1994). Clathrin-dependent localization of α-1,3-mannosyltransferase to the Golgi complex of *Saccharomyces cerevisiae*. *J. Cell Biol*. **127**, 667-678.

Harding, T. M., Morano, K. A., Scott, S. V. and Klionsky, D. J. (1995).

Isolation and characterization of yeast mutants in the cytoplasm to vacuole protein targeting pathway. *J. Cell Biol.* **131**, 591-602.

Harding, T. M., Hefner-Gravink, A., Thumn, M. and Klionsky, D. J. (1996). Genetic and phenotypic overlap between autophagy and the cytoplasm to vacuole protein targeting pathway. *J. Biol. Chem.* **30**, 17621-17624.

Hicke, L. 1997. Ubiquitin dependent internalization and down-regulation of plasma membrane protein. *FASEB J.* **11**, 1215-1226.

Hoffman, M. and Chiang, H.-L. (1996). Isolation of degradation-deficient mutants defective in the targeting of fructose-1,6-bisphosphatase into the vacuole for degradation in *Saccharomyces cerevisiae*. *Genetics* **143**, 1555-1566.

Huang, P.-H. and Chiang, H.-L. (1997). Identification of novel vesicles in the cytosol to vacuole protein degradation pathway. *J. Cell Biol.* **136**, 803-810.

Johnson, L. M., Bankaitis, V. A. and Emr, S. D. (1987). Distinct sequence determinants direct intracellular sorting and modification of a yeast vacuolar protease. *Cell* **48**, 875-885.

Jones, E. W. (1991). Three proteolytic systems in the yeast *Saccharomyces cerevisiae*. *J. Biol. Chem.* **266**, 7963-7966.

Kaiser, C. A. and Schekman, R. (1990). Distinct sets of SEC genes govern transport vesicle formation and fusion early in the secretory pathway. *Cell* **61**, 723-733.

Kim, J. and Klionsky, D. (2000). Autophagy, cytoplasm-to-vacuole targeting pathways, and pexophagy in yeast and mammalian cells. *Annu. Rev. Biochem.* **69**, 303-342.

Klionsky, D. J. and Ohsumi, Y. (1999). Vacuolar import of proteins and organelles from the cytoplasm. *Annu. Rev. Cell Dev. Biol.* **15**, 1-32.

Klionsky, D. J., Herman, P. K. and Emr, S. D. (1990). The fungal vacuole: composition, function, and biogenesis. *Microbiol. Rev.* **54**, 266-292.

Klionsky, D. J., Cueva, R. and Yaver, D. S. (1992). Aminopeptidase I of *Saccharomyces cerevisiae* is localized to the vacuole independent of the secretory pathway. *J. Cell Biol.* **119**, 287-299.

Kuchler, K., Sterne, R. E. and Thorner, J. (1989). Saccharomyces cerevisiae STE6 gene product: a novel pathway for protein export in eukaryotic cells. *EMBO J.* **20**, 3973-3984.

Kuchler, K. and Thorner, J. (1992). Secretion of peptides and proteins lacking hydrophobic signal sequences: the role of adenosine triphosphate-driven membrane translocators. *Endocr. Rev.* **13**, 499-514.

Marcusson, E. G., Horadovsky, B. F., Cereghino, J. L., Gharakhanian, E. and Emr, S. (1994). The sorting receptor for yeast vacuolar carboxypeptidase Y is encoded by the *VPS10* gene. *Cell* **77**, 579-586.

Michaelis, S. (1993). STE6, the yeast a-factor transporter. *Semin. Cell Biol.* **4**, 17-27.

Raymond, C. K., Howald-Stevenson, I., Vater, C. A. and Stevens, T. H. (1992). Morphological classification of the yeast vacuolar protein sorting mutants: evidence for a prevacuolar compartment in class E vps mutants. *Mol. Biol. Cell* **3**, 1389-1402.

Robinson, J. S., Klionsky, D. J., Banta, L. M. and Emr, S. D. (1988). Protein sorting in *Saccharomyces cerevisiae*: isolation of mutants defective in the delivery and processing of multiple vacuolar hydrolases. *Mol. Cell. Biol.* **8**, 4936-4948.

Rothman, J. and Stevens, T. (1986). Protein sorting in yeast: mutants defective in vacuolar biogenesis mislocalize vacuolar proteins into the late secretory pathway. *Cell* **47**, 1041-1051.

Scott, S. V., Hefner-Gravink, A., Morano, K. A., Noda, T., Ohsumi, Y. and Klionsky, D. J. (1996). Cytoplasm to vacuole targeting and autophagy employ the same machinery to deliver proteins to the yeast vacuole. *Proc. Natl. Acad. Sci. U.S.A.* **93**, 12304-12308.

Shieh, H.-L. and Chiang, H.-L. (1998). In vitro reconstitution of glucose-induced targeting of fructose-1,6-bisphosphatase into the vacuole in semi-intact yeast cells. *J. Biol. Chem.* **273**, 3381-3387.

Shieh, H.-L., Chen, Y., Brown, C. R. and Chiang, H-L. (2001). Biochemical analysis of fructose-1,6-bisphosphatase import into vacuole import and degradation vesicles reveals a role for *UBC1* in vesicle biogenesis. *J. Biol. Chem.* **276**, 10398-10406.

Shintani, T., Suzuki, K., Kamada, Y., Noda, T and Ohsumi, Y. (2001). Apg2p functions in autophagosome formation on the perivacuolar structure. *J. Biol. Chem.* **276**, 30452-30460.

Takeshige, K., Baba, M., Tsuboi, S., Noda, T. and Ohsumi, Y. (1992). Autophagy in yeast demonstrated with proteinase-deficient mutants and conditions for its induction. *J. Cell Biol.* **119**, 301-311.

Tsukada, M. and Ohsumi, Y. (1993). Isolation and characterization of autophagy-defective mutants of *Saccharomyces cerevisiae*. *FEBS Lett.* **333**, 169-174.

Tuttle, D. L. and Dunn, W. A. (1995). Divergent modes of autophagy in the methylotrophic yeast *Pichia Pastoris*. *J. Cell Sci.* **108**, 25-35.

Valls, L. A., Hunter, C. P., Rothman, J. H. and Stevens, T. H. (1987). Protein sorting in yeast: the localization determinant of yeast vacuolar carboxypeptidase Y resides in the propetide. *Cell* **48**, 887-897.

Yoshihisa, T. and Anraku, Y. (1990). A novel pathway of import of α-mannosidase, a marker enzyme for vacuolar membrane, in *Saccharomyces cerevisiae*. *J. Biol. Chem.* **265**, 22418-22425.